

Monte Carlo Modeling of Photon Interrogation Methods for Characterization of Special Nuclear Material

S. Clarke^{*1}, S. A. Pozzi², E. Padovani³ and T. J. Downar¹

¹*School of Nuclear Engineering, Purdue University, West Lafayette, IN 47907*

²*Oak Ridge National Laboratory, Oak Ridge, TN 37831*

³*Department of Nuclear Engineering, Polytechnic of Milan, Milan, Italy*

Abstract

This work illustrates a methodology based on photon interrogation and coincidence counting for determining the characteristics of fissile material. The feasibility of the proposed methods was demonstrated using a Monte Carlo code system to simulate the full statistics of the neutron and photon field generated by the photon interrogation of fissile and non-fissile materials. Time correlation functions between detectors were simulated for photon beam-on and photon beam-off operation. In the latter case, the correlation signal is obtained via delayed neutrons from photofission, which induce further fission chains in the nuclear material. An analysis methodology was demonstrated based on features selected from the simulated correlation functions and on the use of artificial neural networks. We show that the methodology can reliably differentiate between highly enriched uranium and plutonium. Furthermore, the mass of the material can be determined with a relative error of about 12%.

Keywords: MCNP, MCNP-PoliMi, Artificial neural network, Correlation measurement, Photofission

1. Introduction

Several recent efforts have focused on the development of new measurement systems for the identification of nuclear material enclosed in shielded containers; this research has applications in the areas of nonproliferation and homeland security [1] - [3]. The detection of shielded highly enriched uranium is particularly challenging because uranium, in contrast to the even-numbered plutonium isotopes, has a very low spontaneous fission rate. As a consequence, it becomes important to investigate active interrogation methods based on neutron or gamma ray sources. The development of these types of measurement systems includes selecting the interrogation source and the neutron and/or gamma ray radiation detectors. Currently, the following detectors are widely used, with various degrees of success: helium-3 for the detection of neutrons, high purity germanium detectors, sodium iodide, and cadmium zinc telluride for the detection of gamma rays, and plastic and liquid scintillation systems for the detection of neutrons and gamma rays.

In this paper, we propose a measurement system that is based on coincident counting of neutrons and gamma rays from the photon interrogation of nuclear materials. The use of a photon interrogation source (instead of neutrons) has the advantage of a greater penetrability in low-Z materials typically used as industrial packing; therefore, fissile material shielded in such cargos may be more readily interrogated. To determine the feasibility and sensitivity of such a measurement system, we have developed a Monte Carlo code system consisting of modified versions of the codes MCNPX and MCNP-

*Corresponding author, Tel.: 765/494-7828, Fax. 765/494-9570, E-mail: clarkesd@purdue.edu

PoliMi. The codes simulate the neutron and photon fields generated during the interrogation of fissile (and non-fissile) material with a high-energy photon source (of the order of 10 MeV). Photo-atomic and photo-nuclear collisions are modeled, and time-correlated detections are computed both for photon beam-on and photon beam-off operation. The signal obtained in photon beam-on operation consists of correlated particles emitted by the primary photofissions. The signal obtained in photon beam-off operation consists of correlated particles emitted by secondary fissions induced by the delayed neutrons from the primary photofissions. To our knowledge, a Monte Carlo code capable of simulating these physical quantities is not currently available.

Photofission is similar to neutron-induced fission in that it begins with the formation of a compound nucleus which then undergoes a series of large vibrations that overcome the nuclear force causing the nucleus to fission into two fragments. At the instant of fission, the two fission fragments are left in a highly excited state. Multiple “prompt” neutrons and photons are emitted almost instantaneously and the two nuclei reach the ground state, from which chains of successive beta decays begin. As a result of some of these decays, a small fraction of “delayed” neutrons are emitted, over a period of up to several minutes, with an intensity falling off rapidly with time. In a fissile assembly, the probability that photofission will occur following irradiation with the photon beam of a given energy is governed by the reaction cross-sections shown in Figure 1 [4].

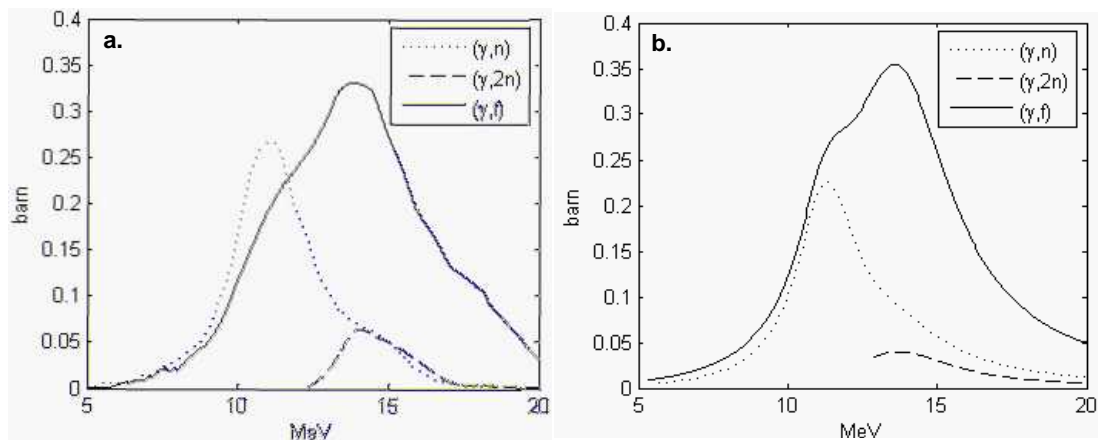


Figure 1. Photonuclear cross-sections for U-235 (a) and Pu-239 (b).

The presence of correlated particle emissions originating from fission chains generates a correlation signal that contains *unique* indicators of the occurrence of fission, and thus of the presence of nuclear materials. The proposed measurement technique is based on the acquisition of these correlated events by appropriate neutron and gamma ray detectors. The proposed technique will provide a more robust indication of the presence of nuclear materials than the measurement of count rates alone. In fact, the signal from the nuclear material will be more readily distinguished from the background, which consists for the most part of uncorrelated events. In addition, it is expected that this technique will lead to more sophisticated analyses with enhanced sensitivity for the measurement of the characteristics of fissile materials.

2. Monte Carlo Simulations

2.1. Description of MCNP-PoliMi Code System

Monte Carlo codes have been widely used to design and analyze measurements such as those considered here; however, when modeling the time-correlated events resulting from photon interrogation, the widely-used Monte Carlo code MCNP-X has some limitations. Specifically, when considering a single interaction, MCNP-X deviates from physical reality and the particles resulting from photonuclear interactions are not modeled correctly on an event-by-event basis [5].

A modified version of MCNP4c called MCNP-PoliMi has been recently developed to simulate time-analysis quantities and to include a correlation between individual neutron interactions and corresponding photon production [6], [7]. MCNP-PoliMi is capable of running with all standard MCNP source types and includes definitions for several specific spontaneous fission sources. In the new version of the code used to treat photonuclear events, a source file is generated using a modified version of MCNP-X and read by MCNP-PoliMi. This source file is generated by simulating the interrogation of fissile material by the photon beam and recording relevant information on all photonuclear events, including photofission, (γ, n) and $(\gamma, 2n)$ reactions. The information that is recorded to file includes the location, number of neutrons and gamma rays emitted, as well as the energy and direction of the emitted particles. This source is read by MCNP-PoliMi and the particles are transported through the system and into the detectors.

A detector-specific post-processing script is then used to analyze the results from MCNP-PoliMi; this script models the detector response and computes several statistical quantities of interest, among which are the time correlation functions used in this work. The general behavior of a typical detector-detector correlation function is illustrated in Figure 2. The two main features of correlation functions are the central and secondary peaks; the central peak occurs at time zero as a result of two fission gamma rays arriving in exact coincidence. The secondary peaks are a consequence of a fission neutron arriving in coincidence with a gamma. Because the neutron velocity depends on the neutron energy, and is always smaller in magnitude than the gamma velocity, the secondary peaks are broader and occur at a time greater than zero. There are two characteristic *wings* visible in the beam-off curves on either side of the (γ, γ) peak known as cross-talk peaks. These peaks result from prompt fission gammas scattering from one detector to the other. The cross-talk peaks are obscured in the beam-on function due to the larger number of neutron-neutron counts.

Figure 2 shows both photon beam-on and photon beam-off correlation functions. The beam-on curve is a result of those fission reactions induced directly by the source photons together with a smaller contribution from neutron-induced fissions. However, when the beam is turned off, the dominating effect of the direct fission is removed; the resulting fission signature is initiated by delayed neutrons. These delayed neutrons are produced from the decay of the fragments of the primary fission on a time scale such that they may be detected after the interrogating source is off*. Such behavior is characteristic to fissile material and will prove instrumental in its identification in the presence of other materials.

*There are also other ways of emission of delayed neutrons; for instance the decay of ^{17}N . This nuclide is produced via the reaction (γ, p) on ^{18}O , with a reaction threshold of 15.9 MeV.

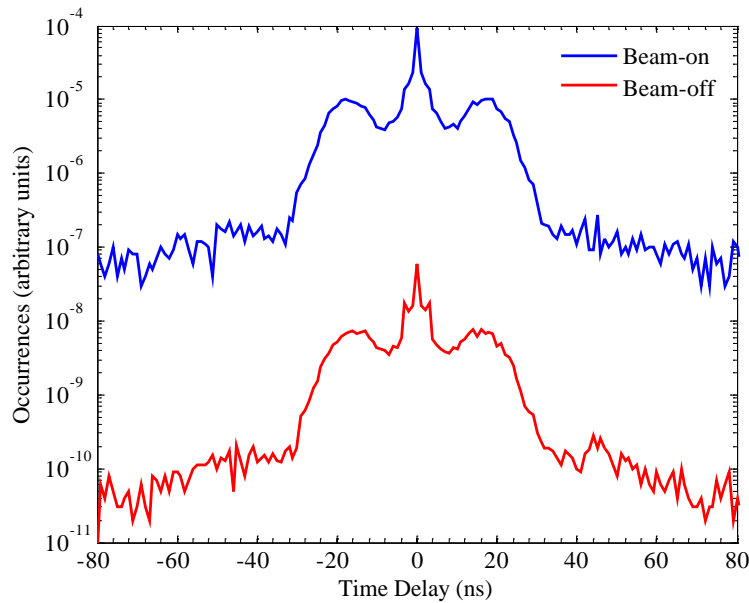


Figure 2. Sample detector-detector correlation function for a bare 1 kg uranium sphere.

2.2. Monte Carlo Model

Simulations were performed using the modified versions of the codes MCNPX and MCNP-PoliMi. The codes simulate the neutron and photon field generated by interrogating fissile (and non-fissile) material with a high energy photon source. In the simulations performed here, 15 MeV photons were used to interrogate the fissile material in two configurations: bare and concealed inside some shielding material. Two detectors were used to capture the radiation emitted by induced photofission in the fissile material; the Monte Carlo model for this detection setup is shown in Figure 3. The radius of the spherical SNM samples ranged from 2.29 cm to 4.99 cm; therefore the minimum separation between the target material and the detectors is 25 cm. The detectors dimensions are 50 by 50 by 10 cm.

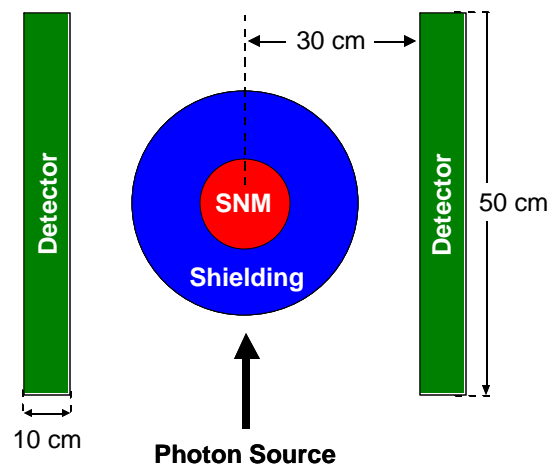


Figure 3. Model geometry for varying masses (radii) of shielded SNM (not to scale).

2.3. Parametric Cases

The range of parametric cases chosen for this work consisted of bare and shielded nuclear material of varying mass; specifically, highly enriched uranium (90% U-235) and plutonium (90% Pu-239) with masses ranging from 1 - 10 kg were considered. An important limiting factor in the cases that can be realistically modeled is the criticality of each configuration; the effective multiplication factor, k_{eff} , of the material should be less than 0.90. A criticality calculation for each bare configuration was performed using MCNP; from these results, it was clear that plutonium masses greater than 6.0 kg have a k_{eff} too high for practical consideration here ($k_{\text{eff}} \geq 0.9$). Each of these fissile masses was then interrogated in both a bare and shielded configuration. The shielding material was chosen to be CelotexTM ($\rho = 0.4 \text{ g/cm}^3$) because it is a common industrial packing material. The thickness of shielding material was chosen on the basis of the mean free path of 2 MeV neutrons (approximate energy of prompt fission neutrons) in CelotexTM. This distance was computed using a simple MCNPX model, and the mean free path was determined to be 18.25 cm.

Figure 4 shows a comparison of correlation functions of four specific cases within the chosen parametric space. Both bare and shielded configurations are shown for 1.0 kg uranium and plutonium spheres; here the shielding is 20.0 cm of CelotexTM. From these figures it is clear that significant differences exist in the correlation function of uranium as compared to plutonium; furthermore, the correlation function of a shielded sample clearly differs from the correlation function of the corresponding bare sample. The first feature to notice is that the overall width of the function is greater for the shielded configurations. This effect is due to neutron attenuation in the shielding material: the scattered neutrons arrive at the detector later, resulting in a wider function. Also, the overall magnitude of the plutonium function is greater than that of the uranium case; this can be attributed to Pu-239 releasing approximately 20% more prompt neutrons per fission event than U-235, while having approximately the same photofission cross section for 15 MeV incident photons according to Figure 1.

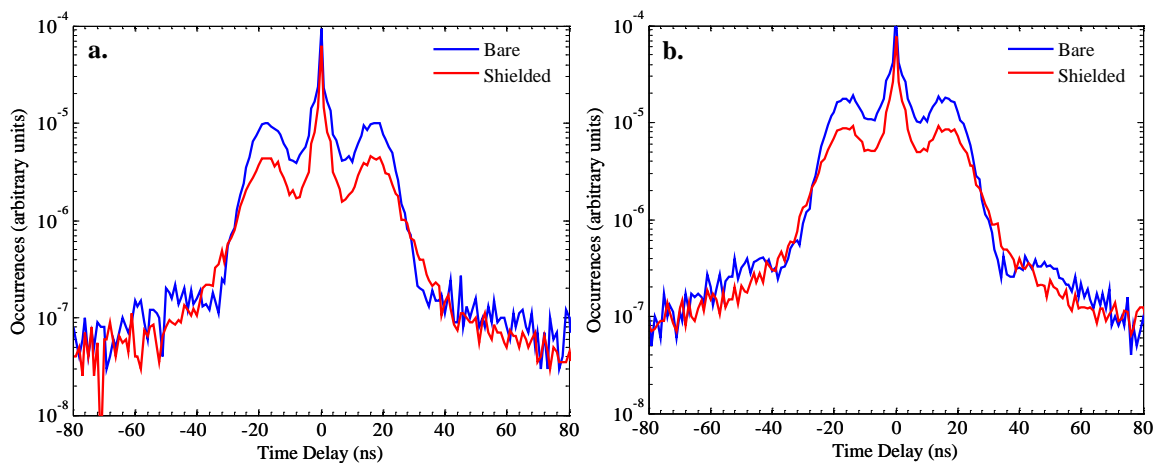


Figure 4. Comparison of beam-on correlation functions for spheres in bare and shielded configurations: a. 1 kg uranium sphere, b. 1 kg plutonium sphere. Shielded cases employ 20 cm of CelotexTM.

2.4. Artificial Neural Network Analysis

The data analysis was performed with a simple three-layer, feed-forward artificial neural network (ANN). An ANN is a system of artificial neurons arranged in layers linked together with weighted transfer functions which can be customized on the basis of the application [8]. Examples of typical transfer functions are linear or sinusoidal functions. The weights associated with each transfer function are determined during the training procedure, whereby the network learns from a large set of examples with known outcomes. A feed-forward, backpropagation network is applied here consisting of three layers: input (5 nodes), hidden (4 nodes) and output layer (2 nodes). A schematic of such an ANN is shown in Figure 5.

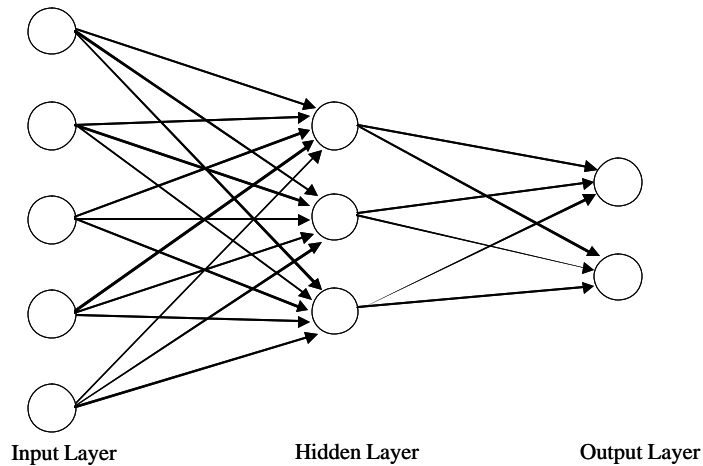


Figure 5. Schematic diagram of a three-layer, feed-forward artificial neural network.

In our application, the input layer consisted of features that are obtained from the simulated correlation functions described in Section 2.1, and the output layer consisted of the desired information on the fissile material. The training was performed on a set of simulated results from a variety of material configurations. Once trained, the neural network was ready to analyze unknown fissile samples.

The input and output features were taken directly from the simulated correlation functions. In the practical case of data from a field measurement, the central peak during beam-on operation would be obscured due to detector saturation from photo-atomic events. Therefore the central peak was not used in the data analysis and more emphasis was placed on the beam-off correlation function. The input and output variables for the updated network are listed in Table 1 and illustrated in Figure 6.

Table 1. Input and output variables for the ANN.

Inputs	Outputs
1. Beam-off (γ, γ) peak height	1. Material type
2. Ratio of beam-off (γ, γ) and (γ, n) peaks	2. Material mass
3. Ratio of beam-on to beam-off (γ, n) peaks	
4. Beam-on, full-width-50 th (γ, n) max time	
5. Beam-off, full-width-50 th (γ, n) max time	

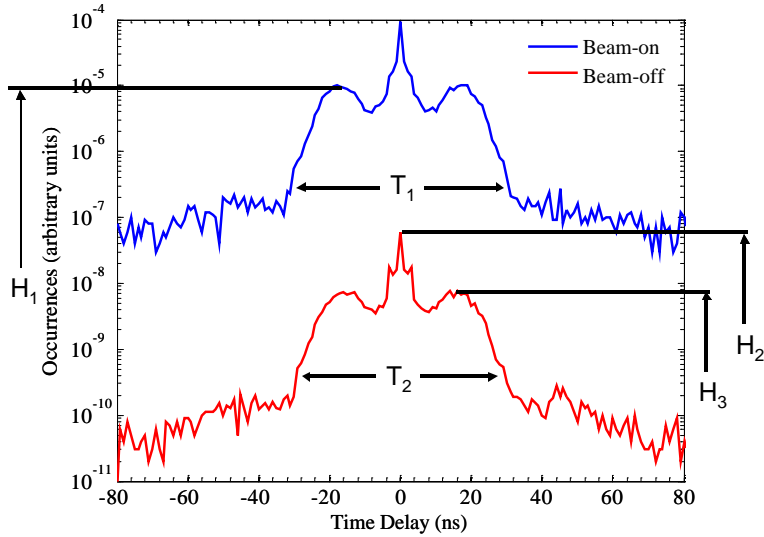


Figure 6. Sample correlation functions illustrating the features chosen as inputs for the ANN.

Each of these input variables was plotted as a function of mass for both uranium and plutonium in order to understand the underlying physics and determine the feasibility of an ANN. Figure 7 shows the trend of input variables 1 – 4; the width of the beam-off curve is not interesting as it follows the same trend as the beam-on data shown.

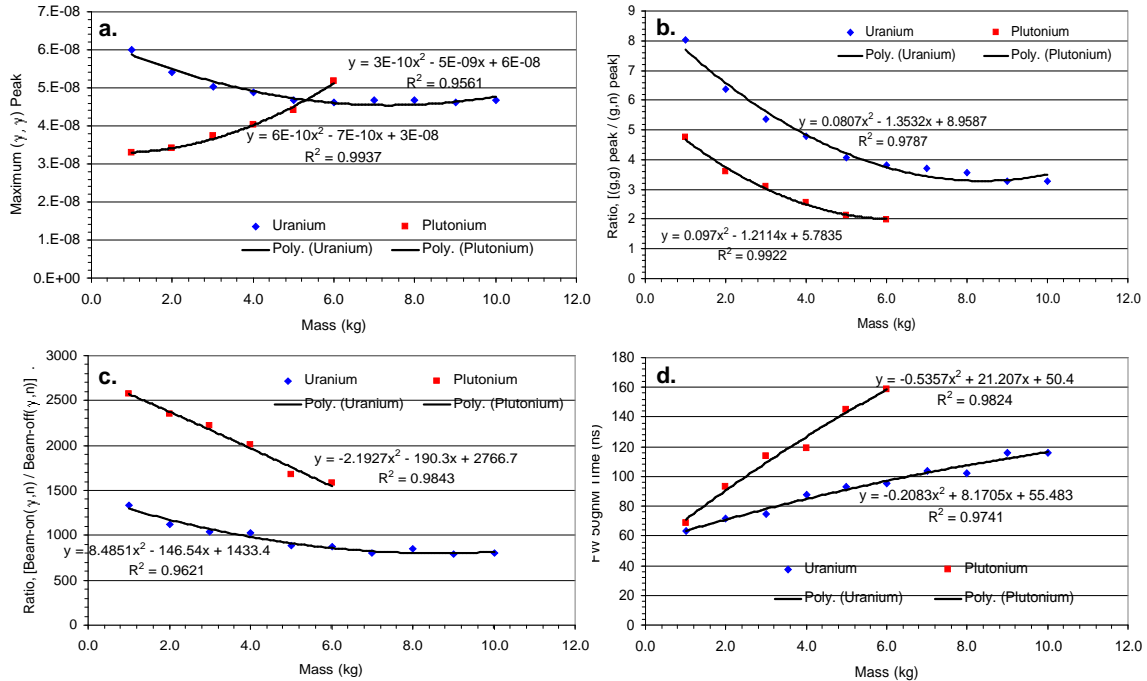


Figure 7. ANN input variables 1 – 4 plotted as a function of mass of bare uranium and plutonium spheres

All of the trends displayed in Figure 7b, c, and d are as expected when one considers that the effective multiplication factor of each of the samples varies nearly linearly with mass with plutonium being approximately twice as critical at a given mass. In Figure 7a. the uranium and plutonium data are seen to intersect around 5 kg; furthermore, the (γ, γ) peak maximum as plotted decreases for uranium and increases for plutonium. There are

two governing physical phenomena here: increased source multiplication and increased self-shielding. For plutonium, the incremental criticality increase is greater than the incremental increase in self-shielding; the opposite is true for uranium due to the small k_{eff} of the samples ($k_{\text{eff}} = 0.59522$ for 10 kg uranium and $k_{\text{eff}} = 0.50141$ for 1 kg plutonium).

In order to construct a data set large enough to train the ANN, second-order polynomials were fit to each of these curves. A new training set was then built using these polynomials. The range of the training data represents the full data range in steps of 0.10 kg.

3. Results

The ANN was trained and tested using the polynomial approximations of the simulated measurements from the 16 bare cases; this resulted in 142 independent training points. The ANN was trained and converged fully after 1,000 cycles. Testing was then performed using the original 16 data points. The test results are shown in Figure 8 and Figure 9 for material type and mass, respectively.

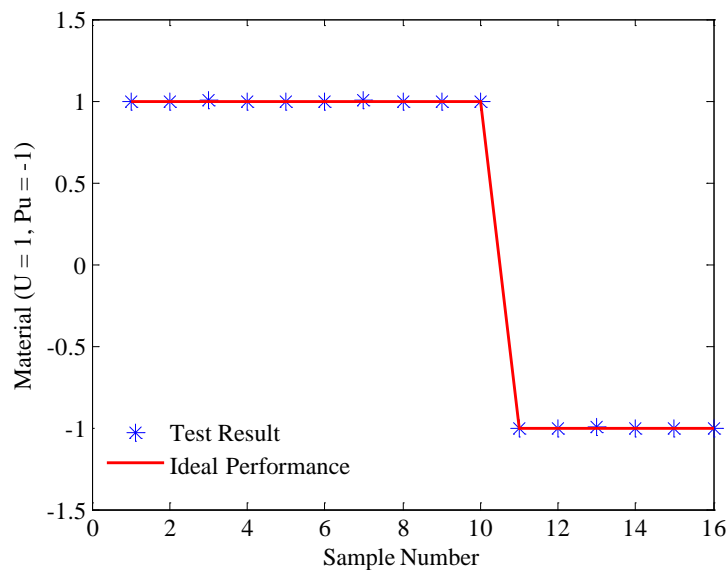


Figure 8. Test results for material type using a three-layer feed-forward ANN.

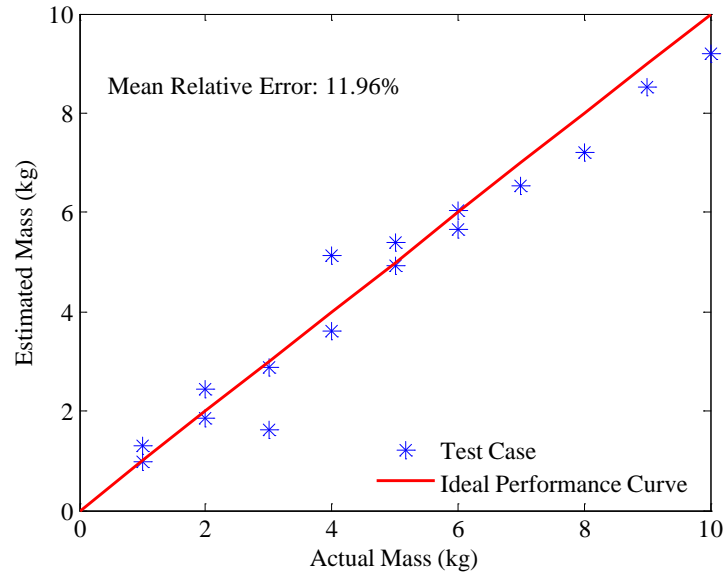


Figure 9. Test results for material mass using a three-layer feed-forward ANN.

Figure 8 shows the test results for material type where +1 and -1 are used to denote uranium and plutonium, respectively; excellent agreement is observed in all cases. The prediction of sample mass is shown to be correct to a MAPE of 11.96 for unshielded cases only.

4. Summary and Conclusions

We have shown that a methodology based on photon interrogation and coincidence counting has potential for determining the characteristics of shielded fissile materials. The analysis was based on combined stochastic and artificial intelligence methodologies. We developed and implemented modifications to Monte Carlo codes in order to simulate the active interrogation of concealed fissile material using a photon interrogation source and coincidence counting. We then used this tool to simulate the photon interrogation of bare and shielded highly enriched uranium and plutonium spheres of varying mass. The simulations consisted of fissile material placed between two plastic scintillation detectors with a 15 MeV mono-energetic photon interrogation source. The shielding consisted of 20 cm of moderating material with a density of 0.4 g/cm^3 . The data analysis was performed using an artificial neural network, which predicted the material type with 100% accuracy and the mass of the SNM samples with a mean error of about 12%.

We believe that the implemented system can be extended to simulate a wider range of input scenarios. Specifically, in the continuing development of this analysis algorithm we will consider a variety of shielding materials at increasing thicknesses. Realistic source of photons should also be considered; for example bremsstrahlung X-rays of endpoint energy 15 to 25 MeV, or 6 to 7 MeV gamma rays coming from (p, γ) reaction on F-19. Some improvements to the distributions of neutrons and photons emitted in both neutron- and photon-induced fission can be still implemented in MCNP-PoliMi. An extended output file and improved post-processing are needed if we wish to simulate the occurrence of accidental correlated counts. These improvements will enable us to model realistic-scale models and validate the proposed system for field deployment.

References

- [1] C.E. Moss, C.L. Hollas, G.W. McKinney, and W.L. Meyers (2005). *Comparison of Active Interrogation Techniques*, Nuclear Science Symposium and Medical Imaging Conference, October 23-29, 2005, San Juan, Puerto Rico.
- [2] Walter Hage (2005). *Nondestructive Fissile Material Assay by Induced Fission Neutron Correlation*, Nucl. Instr. and Meth. A, **551**: 396-419.
- [3] J.T. Mihalcz, J.A. Mullens, J.K. Mattingly and T.E. Valentine (2000). *Physical Description of Nuclear Materials Identification System (NIMS) Signatures*, Nucl. Instr. And Meth. A, **450**: 531-555.
- [4] IAEA Photonuclear Data. *Photonuclear Evaluations and Plots*. <http://t2.lanl.gov/data/photonuclear.html> (31 May 2006).
- [5] X-5 Monte Carlo Team (2003). *MCNP - A General Monte Carlo N-Particle Transport Code, Version 5, vols 1 - 3*. Los Alamos National Laboratory. LA-UR-03-1987, LA-CP-03-0245, and LA-CP-03-0284.
- [6] S. A. Pozzi, E. Padovani, and M. Marseguerra (2003). *MCNP-PoliMi: A Monte Carlo Code for Correlation Measurements*, Nucl. Instr. and Meth. A, **513**: 550-558.
- [7] S. A. Pozzi, E. Padovani, and M. Monville, *Nuclear Materials Identification by Photon Interrogation*, Mathematics and Computations 2005, September 12-15, 2005, Avignon, France.
- [8] Lefteri H. Tsoukalas and Robert E. Uhrig (1997). *Fuzzy and Neural Approaches in Engineering*. John Wiley and Sons, Inc, New York, NY.